Hindawi
Mathematical Problems in Engineering
Volume 2021, Article ID 5747768, 8 pages
https://doi.org/10.1155/2021/5747768

Research Article

Study on the Effect of Precrack on Specimen Failure Characteristics under Static and Dynamic Loads by Brazilian Split Test

Enyan Liu,[1] Fuchun Liu,[1] Youwei Xiong,[1] Xianquan Lei,[1] and Shiming Wang[2]

[1]*CINF Engineering Co., Ltd., Changsha, Hunan 410000, China*
[2]*School of Civil Engineering, Hunan University of Science and Technology, Xiangtan, Hunan 411201, China*

Correspondence should be addressed to Shiming Wang; wang_shiming@hnust.edu.cn

Received 8 May 2021; Accepted 8 July 2021; Published 20 July 2021

Academic Editor: Łukasz Jankowski

To analyse the dynamic failure characteristics of the rock with a crack in rock engineering, the Brazilian split tests were conducted on the split Hopkinson pressure bar (SHPB) using precrack specimens under dynamic loads. In the study, five groups of different precrack angles are selected; they are 0°, 30°, 45°, 60°, and 90°, respectively. The results show that the static failure load of the specimen as a whole decreases to increase with the growth of the loading angle, and the *DIF* linear increases with the increase of the loading rate; the failure load of the specimen with an angle of 45° precrack is the most sensitive to the loading rate, followed by 0°, 60°, 30°, and 90°. The crack initiation time of specimen with 30°, 45°, and 60°precrack decreases with the loading rate, while it has no obvious change with the loading rate with 0° and 90°precrack. The failure mode of the specimen was controlled by the stress concentration at the crack tip; the main cracks all point from the crack tip to the loading end. When the precrack and the loading direction are at a certain angle, the failure process will produce secondary cracks; it would be particularly obvious under dynamic load splitting. Once the precrack and the loading direction are at a certain inclination angle, type-II secondary cracks will develop under dynamic load splitting.

1. Introduction

In actual rock masses, there are still many defects such as natural cracks and artificial cracks of different scales inside the rock mass. These defects are one of the main internal factors that affect the mechanical properties of rock mass deformation and strength. As we know, the tensile strength of rock is an important indicator of rock mechanical properties. In actual engineering, most of the rocks are damaged by tension. Therefore, studying the failure characteristics of cracked rocks under tension is of great significance to engineering practice.

The Brazilian split test is the most common method to test the tensile properties of rock mechanics. With the widespread application of the Brazilian test, various improved forms of disc specimens have been developed. Wang et al. [1, 2] verified the feasibility of the improved platform disc specimen based on the marble split test. For Brazilian disc specimens with precrack, by changing the angle of the precracks, different modes of crack propagation can be known. At present, a lot of research has been carried out on the failure characteristics of rock-like materials with crack using the Brazilian split test. The influence of the strain rate on dynamic fracture of rock was studied by using disk specimens with holes and grooves [3]. Combining experiments and numerical simulations, the fracture law of discs of rock-like materials under the influence of single cracks and double cracks at different angles are studied by Haeri et al. [4]. Zhou and Wang [5] used a numerical simulation method to study the influence of specimen size and crack inclination on the peak failure load of the precrack Brazilian disc specimen. Based on the phase-field method model (PFM), the crack propagation law of the precracked Brazilian disc specimens with different widths and angles is

simulated [6]. Wang et al. [7] conducted Brazil on a disc specimen with prefabricated cracks to study the fracture characteristics and failure mechanism of black shale under the combined action of split test-bedding and precracks. Zhou et al. [8] studied the influence of the natural filling fracture on crack propagation by using precrack Brazilian discs with different loading angles.

In summary, the previous Brazilian splitting experiments on cracked rocks were mainly limited to static load or low-frequency dynamic load. In rock underground engineering, blasting excavation is currently the most economical and most common method. Rocks are always disturbed by blast impact and mechanical loads and other dynamic loading during drilling and blasting excavation or the excavation disturbance of the surrounding directors [9–15]. As the SHPB is one of the ideal equipment frequently used to test the dynamic mechanical properties of rocks. This equipment can realize uniaxial impact [16, 17] and three-dimensional complex loading conditions [18–20]. Therefore, for research on the influence of precrack on specimen failure characteristics under dynamic load, a modified 50 mm-diameter SHPB testing device [21] was adopted to conduct the Brazilian split test on red sandstone with precrack. The angles of precrack with the loading direction are 0°, 30°, 45°, 60°, and 90°, respectively, and a set of comparative experiments were carried out at the same time.

2. Experiment Procedures

2.1. Specimens' Preparation. A red sandstone precrack specimen was adopted to be tested in this study, and the size of $\Phi 50\,\text{mm} \times 25\,\text{mm}$ was selected. The precrack is cut by water jet cutting, and the length of all specimens in the study is 15 mm, and the width is 1 mm, as shown in Figure 1(a). In order to monitor the crack initiation time of the specimen at a fixed point, we paste a strain gauge 12 mm away from the end in the loading direction, as shown in Figure 1(b).

2.2. Test Methods. In the study, the static splitting tests were conducted on RMT-150, and the dynamic splitting tests were performed on the SHPB experimental device, as shown in Figure 2. Five sets of precrack static load and dynamic load Brazilian splitting experiments were carried out, and the loading directions were, respectively, 0°, 30°, 45°, 60°, and 90° to the precrack, as shown in Figure 3. According to the test results, three impact levels were selected, namely, 0.35 MPa, 0.4 MPa, and 0.45 MPa impact gas pressure. At the same time, for comparison, a set of Brazilian splitting experiments without precracked specimens were carried out. Moreover, the details of the test are shown in Table 1. Based on SHPB test criteria, the experimental data is valid only when the load of the incident bar end and the transmission bar end are balanced; that is, the load balance at both ends of the specimen is achieved, realizing quasi-static loading [21, 22]. We can see from Figure 4 that, after the stress wave propagates about back and forth about 3 times, about 45 μs, the load on both ends of the specimen reaches equilibrium and lasts about 125 μs. Then, the loading wave value exceeds that of the specimen, and it is destroyed; after that, the contact at the end of the incident bar with the specimen and the end of the transmission bar with the specimen is greatly different, resulting in different loads at both ends. In general, in this process, the load at both ends of the specimen has been balanced before it is broken, and the validity of the test is guaranteed. The resulting loading and loading rate can be calculated by equations (1) and (2):

$$F = \frac{A_e}{2} E_e \left[\varepsilon_i(t) - \varepsilon_r(t) + \varepsilon_t(t)\right], \tag{1}$$

$$\dot{F} = \frac{F_{\max}}{t_1}, \tag{2}$$

where A_e is the area of incident or transmitted bar, E_e is the elastic modulus of the incident or transmitted bar, $F_{\max}$ is maximum load during impact process, and t_1 is the time corresponds to the $F_{\max}$.

3. Result and Analyzes

As there is a precrack in the specimen, the Brazilian splitting stress calculation formula is not applicable. We use the load when the specimen fails to characterize the tensile properties of the rock. Figure 5 shows the influence of precrack on the splitting failure load of the specimen under static load. From Figure 5, we can see that the precrack has a significance on the failure load of the specimen under static load. Compared with the complete specimen, the failure load of the precracked specimen is seriously weakened. With the angle of precrack with loading direction change, the precrack has a different effect on the splitting failure load of the specimen. As the loading angle increases, the failure load of the specimen as a whole decreases to increase. When the precrack is 45°, the splitting failure load of the specimen is the smallest. It is like the results of previous studies [23]. As we know, the failure load of the specimen under dynamic load is affected by the loading rate. Figure 6 shows the variation of *DIF* of precracked specimens with the loading rate under impact loading. As mentioned before, *DIF* in the paper is the ratio of dynamic load to static load. From Figure 6, we can see that the *DIF* has a linear increase relationship with the loading rate. However, the sensitivity of the splitting failure load to the loading rate is different. Among them, the splitting failure load of the specimen with 45°precrack is the most sensitive to the loading rate, followed by 0°, 60°, 30°, and 90° and the intact specimen. This is consistent with the previous view that low-strength concrete shows a relatively large increase in compressive strength under high strain rate loads [24]. It shows that precracks have different effects on the failure load of rock dynamic and static splitting. Compared with static loading, due to the high loading rate, the influence of precracks on failure may be more complicated.

In this test, a strain gauge was attached at 12 mm from the loading end perpendicular to the loading direction to detect crack growth. The crack initiation time can be calculated based on the data recorded by the strain gauge. The initiation time of the crack is from the start point to the

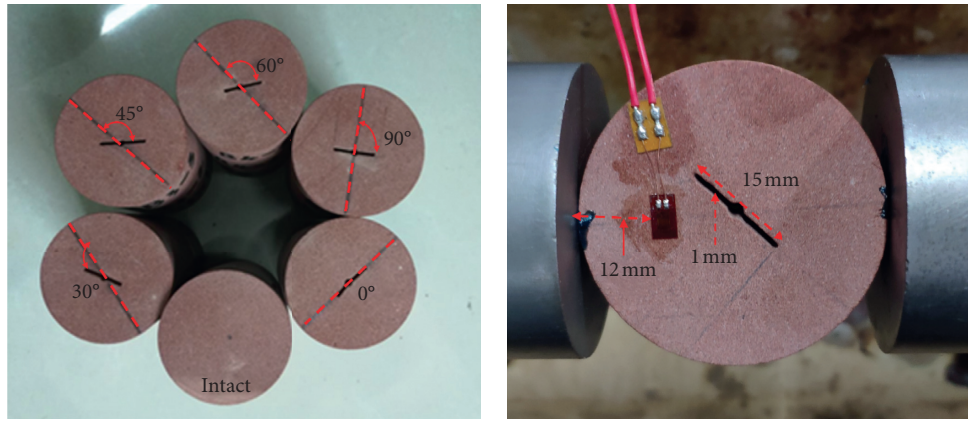

(a) (b)

Figure 1: Rock specimens.

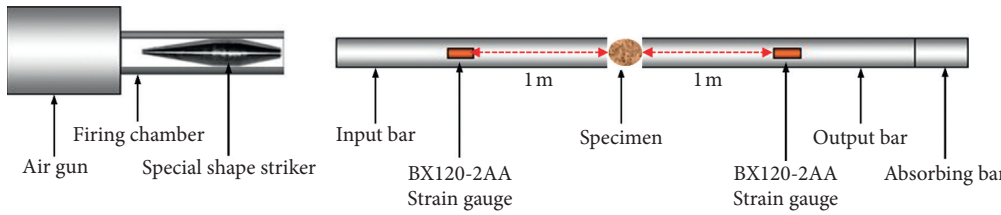

Figure 2: A diagrammatic sketch of SHPB apparatus.

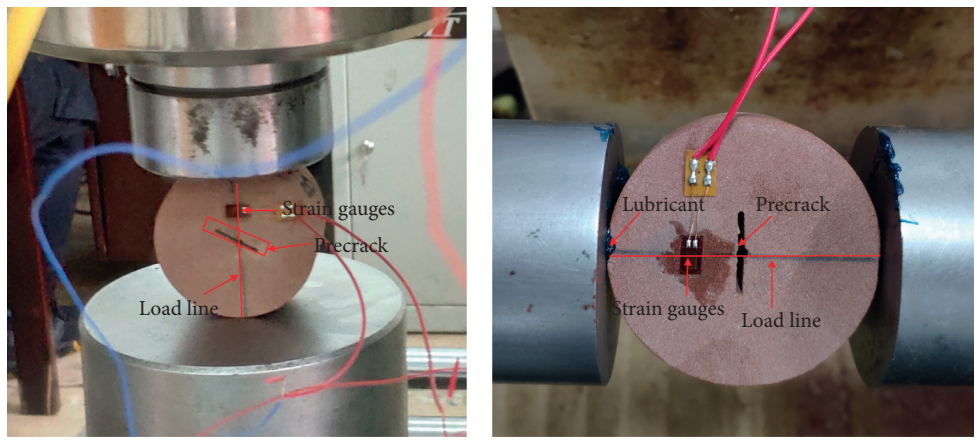

(a) (b)

Figure 3: Detailed loading diagram: (a) static loading and (b) dynamic loading.

Table 1: Testing design for precrack rock specimens.

Precrack angle (°)	Gas pressure (MPa)	Number of specimens	Precrack angle (°)	Gas pressure (MPa)	Number of specimens
0	0.35	3	45	0.45	3
0	0.4	3	60	0.35	3
0	0.45	3	60	0.4	3
30	0.35	3	60	0.45	3
30	0.4	3	90	0.35	3
30	0.45	3	90	0.4	3
45	0.35	3	90	0.45	3
45	0.4	3			

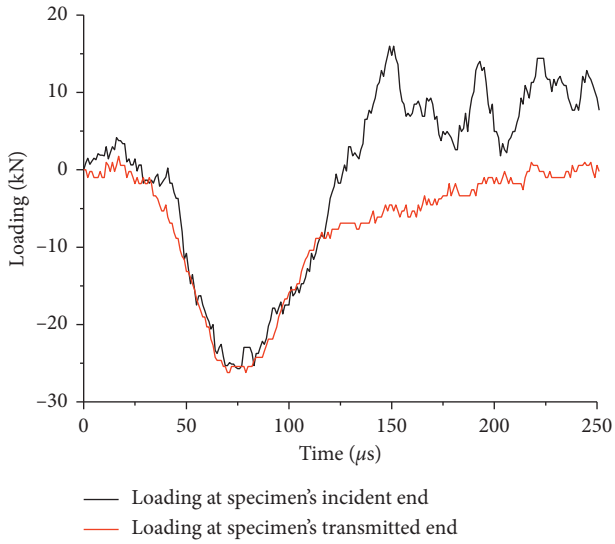

Figure 4: Loading diagram at both ends of the specimen under dynamic loading.

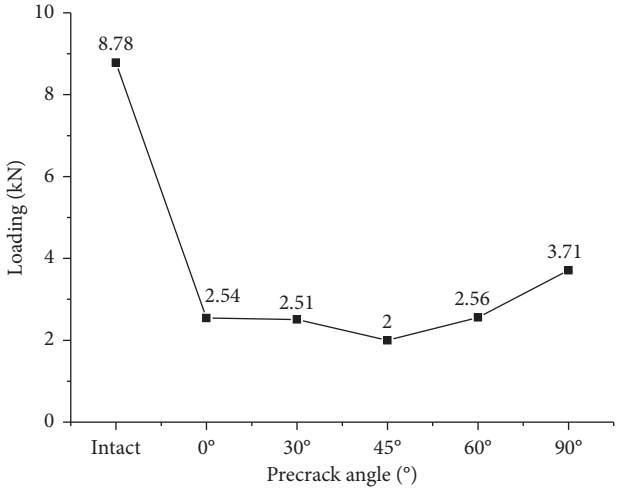

Figure 5: The influence of precracks on the failure load of the specimen under static loading.

endpoint, as shown in Figure 7. In Figure 7, the start point means the test point begins to subject the tensile deformation, and the endpoint means the crack has penetrated the test point. Figure 8 shows the variation of crack initiation time of precrack specimens with the loading rate under dynamic loading. From Figure 8, we can see that, for intact specimens, the crack initiation time decreases as the loading rate increases. At the same time, the crack duration shows two modes with the change of angle of the precrack. When the angles of precrack are 30°, 45°, and 60°, the crack initiation time decreases significantly as the loading rate increases. When the angle of the precrack is 0° and 90°, the crack initiation time varies with the loading rate and does not change significantly.

Figure 9 shows the failure model of the precrack specimen under static loading. From Figure 9, we can see that, under the static load, all specimens fractured along the

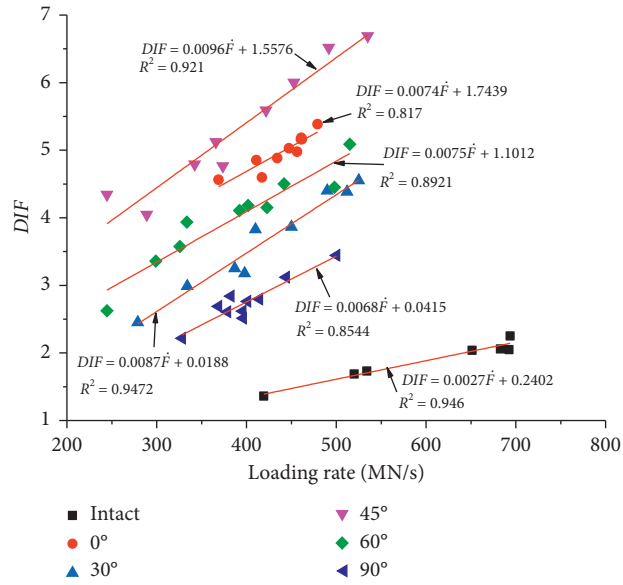

Figure 6: The variation of *DIF* of precracked specimens with the loading rate under dynamic loading.

loading direction. However, the change of the angle of the precrack has a certain degree of the failure model to the rock under splitting conditions. Among them, the failure model of the complete specimen, the 0° precrack specimen, and the 90° precrack specimen are all consistent with the loading direction, as shown in Figures 9(a), 9(b), and 9(f). The failure of the specimen is mainly caused by tensile, and the crack runs through the entire specimen. While the failure model of 30°, 45°, and 60° precrack specimen show shear tension failure, causing the crack to be at a certain angle with the loading line. As a result of the stress concentration at the precrack tip, wing cracks are generated; the appearance time of wing cracks is related to the inclination angle of precrack, and it grows in the form of a curve along the direction of the maximum principal stress. The wing cracks grow steadily as the load increases. The curvature of the wing crack is related to the crack inclination; this is the main crack of failure, and as the load increases, some secondary cracks will occur [6, 8, 25], as shown in Figures 9(c)–9(e). It can be seen from Figure 9 that there are more and obvious secondary cracks near the main crack of the specimen with 30°, 45°, and 60° precrack, and the specimen with 0°, 90°precrack and without precrack do not produce secondary cracks. This is because the different angles make the stress on the precrack tip in complexity; that is, the stress on the precrack tip at 30°, 45°, and 60° are the most complicated. As we all know, rock is more sensitive to dynamic load compare with a static load. The existence of precracks means that there is a stress concentration at the crack tip. The dynamic load will further strengthen the stress concentration at the precrack tip, and at the same time, make the crack propagation direction, not towards the loading direction. Therefore, under dynamic loading, all specimens have main cracks and secondary cracks; all secondary cracks are generated near the precrack tip, and the angle between the secondary crack and the direction of the loading line increases as the angle of the

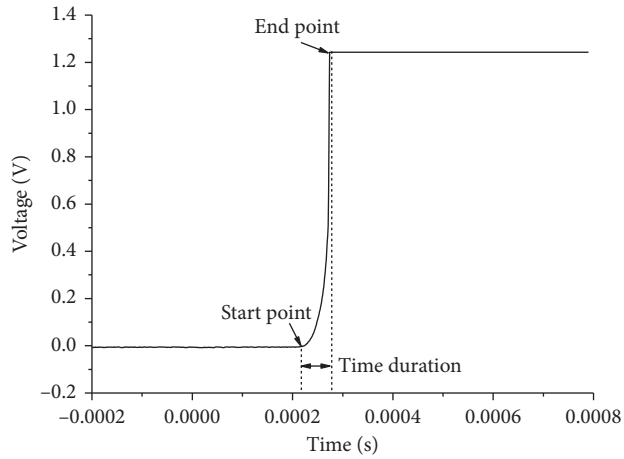

Figure 7: Determination method of crack initiation time.

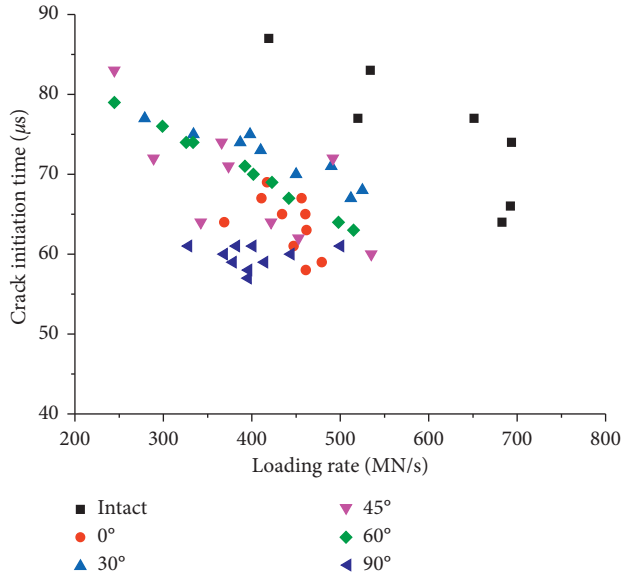

Figure 8: The variation of crack initiation time of precracked specimens with the loading rate under dynamic loading.

precrack increases, as shown in Figure 10. The secondary cracks of the 30°, 45°, and 60° precrack specimens are developed, and the secondary cracks are not always developing in the direction of the main crack.

4. Discussion

Based on the abovementioned experimental results, the precrack has a significant effect on the splitting failure load of the red sandstone under static and dynamic loading. The *DIF* linear increases with the growth of the loading rate. It needs to be pointed out that when the angle of precrack with loading direction is 45°, the failure load under static load is the smallest, while the *DIF* is the largest. The development of secondary cracks is the most obvious in all specimens, no matter under static loading or dynamic loading. Someone pointed out that this phenomenon may be due to the influence of the hole in the specimen, except for precrack tip stress concentration. In this study, as the limitations of the existing equipment, the processing of precrack must be drilled in the middle of the specimen and then cut with water jet cutting. It would be affecting the failure load and failure mode of the specimen. Huang and Yang [23] found that when the crack inclination angle is small, the hole is the main cause of the main crack initiation. When the crack inclination angle is large, the crack becomes the main cause of the main crack initiation. However, from the experimental results of this study, the drill hole has no obvious effect on the failure mode of the specimen. It may be that the diameter of the drill hole in this article is only 2 mm, and no cracks are observed from the periphery of the drill hole in the failure mode of the specimen. Hence, in this study, the failure load and failure mode of the specimen were mainly dominated by the stress concentration at the crack tip. It also proved that the *DIF* is more obvious for brittle materials with low static strength. Compared with static load, as the loading speed is much higher than the static load, the stress concentration at the crack tip is more obvious. The precrack under dynamic load has a more obvious influence on crack development. The crack development is not all oriented in the loading direction, that is, type-II secondary cracks. From Figure 10, we can see that the type-II secondary cracks have developed significantly in the 30°, 45°, and 60° precrack specimen, and the angle of type-II secondary crack with the loading direction increases with the increase of the precrack angle. Therefore, we infer that when the angel of precrack is at a certain inclination angle, under dynamic load splitting, type-II secondary cracks will develop when the specimen is broken. However, these phenomena are difficult to observe under static load.

The failure of the specimen under dynamic loading is dominated by the stress concentration at the precrack tip. For the crack initiation time of the monitoring point, when the precrack is 0° and 90°, the main crack is oriented to the loading direction. The crack is almost along the loading direction, which can be seen in Figure 10, and the crack initiation time does not obviously change with increase of the loading rate. When the precrack is 0°, the crack direction is consistent with the loading direction, and the stress concentration is easier to expand along the loading

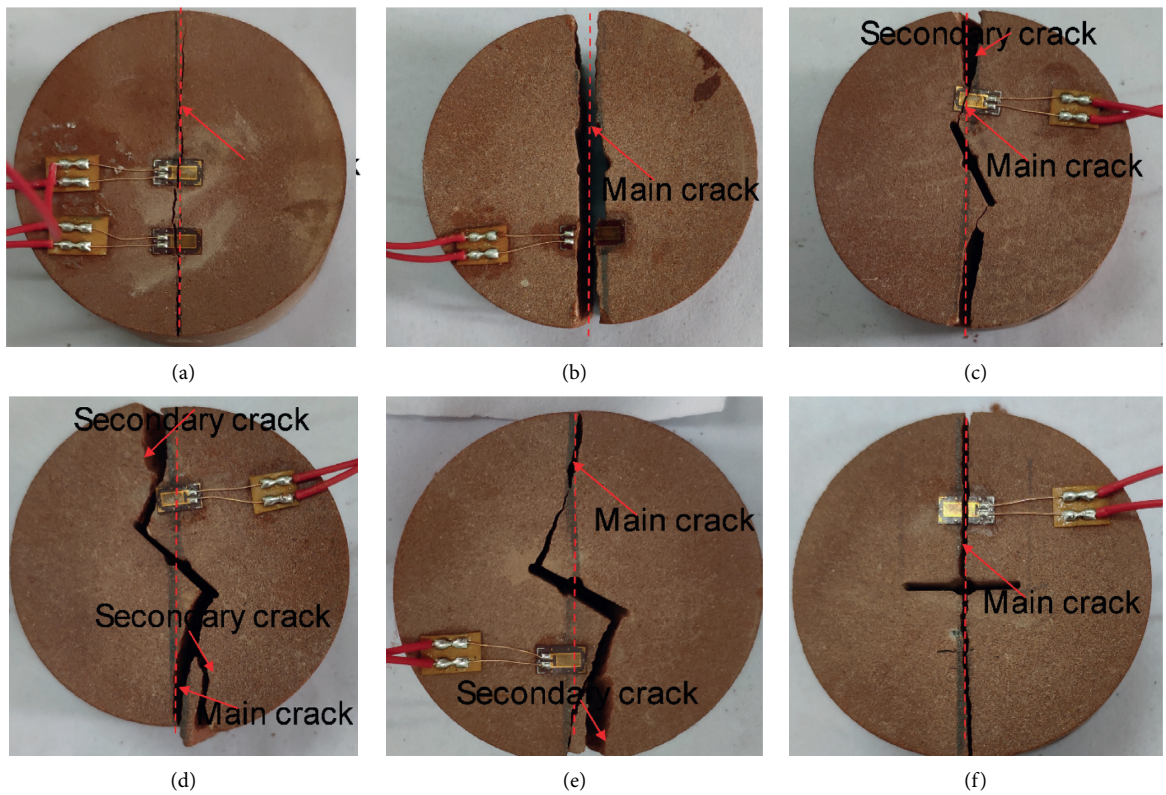

Figure 9: The failure model of precrack specimen under static loading: (a) intact, (b) 0°, (c) 30°, (d) 45°, (e) 60°, and (f) 90°.

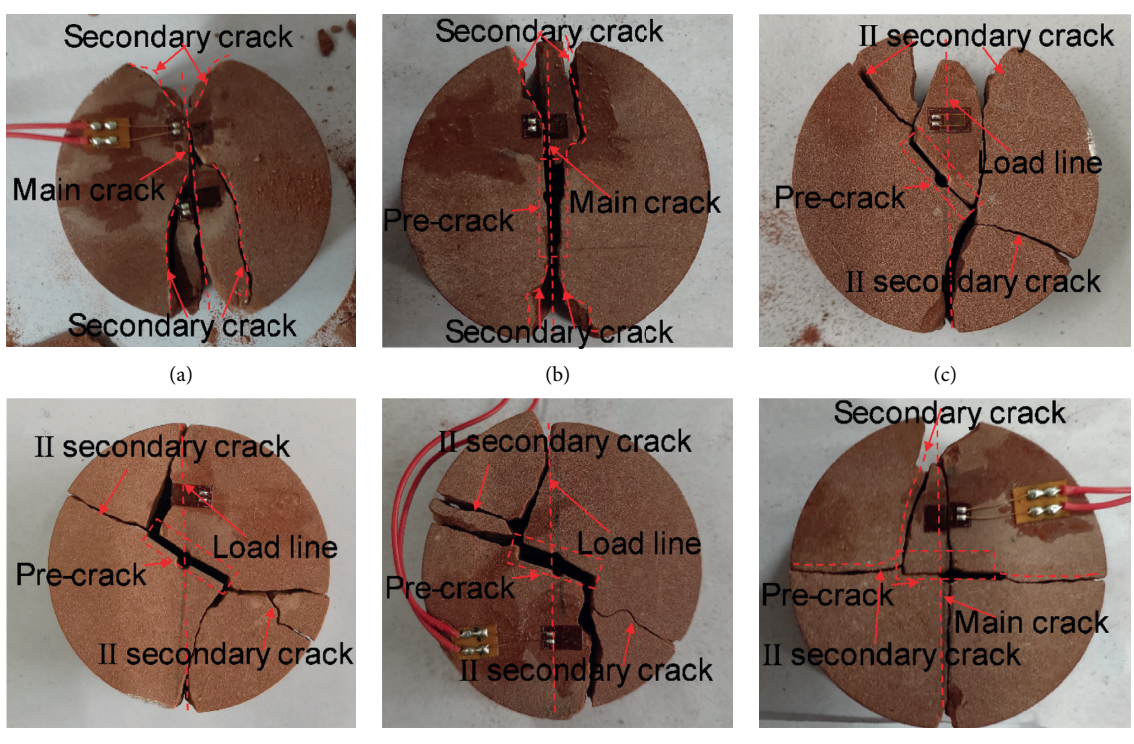

Figure 10: The failure model of precrack specimen under impact loading: (a) intact, (b) 0°, (c) 30°, (d) 45°, (e) 60°, and (f) 90°.

direction. When the precrack is 90°, the precrack is far away from the loading line, and the stress at crack tip coursed by loading is small, resulting in the stress concentration phenomenon is not obvious, so the cracks still propagate from the loading direction. With the inclination of the angle, the failure of the specimen is affected by the combination of loading and stress concentration. The main crack is at a certain angle to the loading direction, resulting in the crack duration decreasing with the increase of the loading rates. The increase of the loading rate shortens the time for the stress concentration at the precrack tip to reach the failure value, thereby affecting the crack initiation time.

5. Conclusion

The dynamic Brazil splitting tests of sandstone were conducted on the SHPB to research the influence of precrack on specimen failure characteristics, and the influence of the angle of precrack with loading direction, loading rate on the failure load, and failure model of red sandstone were analyzed. Moreover, the following main conclusions can be drawn:

(1) The precrack has a significance on the static and dynamic split failure load, and the *DIF* linear increases with the increase of loading rate; the failure load of the specimen with an angle of 45° precrack are the most sensitive to the loading rate, followed by 0°, 60°, 30°, and 90°.

(2) The crack initiation time of specimen with 30°, 45°, and 60° precrack decreases with the loading rate, while it has no obvious change with the loading rate with 0° and 90° precrack.

(3) The failure mode of the specimen was dominated by the stress concentration at the crack tip, particularly obvious under dynamic load splitting. Once the precrack and the loading direction are at a certain inclination angle, type-II secondary cracks will develop under dynamic load splitting.

In this study, the experiment only involves the angle of the crack and does not consider other factors of the crack, such as the length, the location of the distribution, and the thickness of the crack. In the subsequent research, we will further consider these factors and adopt other auxiliary methods, such as DIC, to observe the propagation of cracks and enrich experimental conclusions.

Data Availability

The datasets used during the study are available from the corresponding author upon request.

Conflicts of Interest

The authors declare that they have no conflicts of interest.

Acknowledgments

The work reported here was supported by financial grants from the National Key and Development Program of China (2019YFC1904700, 2016YFC0801600, and 2018YFC0604600).

References

[1] Q. Z. Wang, X. M. Jia, and S. Q. Kou, "The flattened Brazilian disc specimen used for testing elastic modulus, tensile strength and fracture toughness of brittle rocks: analytical and numerical results," *International Journal of Rock Mechanics and Mining Sciences*, vol. 41, no. 2, pp. 245–253, 2004.

[2] Q. Z. Wang and L. Z. Wu, "The flattened Brazilian disc specimen used for determining elastic modulus, tensile strength and fracture toughness of brittle rocks: experimental results," *International Journal of Rock Mechanics and Mining Sciences*, vol. 41, no. 3, pp. 26–30, 2004.

[3] D. E. Lambert and C. Allen Ross, "Strain rate effects on dynamic fracture and strength," *International Journal of Impact Engineering*, vol. 24, no. 10, pp. 985–998, 2000.

[4] H. Haeri, K. Shahriar, M. F. Marji, and P. Moarefvand, "Experimental and numerical study of crack propagation and coalescence in pre-cracked rock-like disks," *International Journal of Rock Mechanics and Mining Sciences*, vol. 67, no. 4, pp. 20–28, 2014.

[5] X. P. Zhou and Y. T. Wang, "Numerical simulation of crack propagation and coalescence in pre-cracked rock-like Brazilian disks using the non-ordinary state-based peridynamics," *International Journal of Rock Mechanics and Mining Sciences*, vol. 89, pp. 235–249, 2016.

[6] S. W. Zhou and C. C. Xia, "Propagation and coalescence of quasi-static cracks in Brazilian disks: an insight from a phase field model," *Acta Geotechnica*, vol. 14, pp. 1195–1214, 2018.

[7] H. Wang, Y. Li, S. Cao et al., "Brazilian splitting test study on crack propagation process and macroscopic failure mode of pre-cracked black shale," *Chinese Journal of Rock Mechanics and Engineering*, vol. 39, no. 5, pp. 912–926, 2020.

[8] J. Zhou, Y. Zeng, Y. Guo, X. Chang, and C. Yang, "Effect of natural filling fracture on the cracking process of shale Brazilian disc containing a central straight notched flaw," *Journal of Petroleum Science and Engineering*, vol. 196, Article ID 107993, 2020.

[9] D. J. Armaghani, M. Koopialipoor, M. Bahri et al., "A SVR-GWO technique to minimize flyrock distance resulting from blasting," *Bulletin of Engineering Geology and the Environment*, vol. 79, no. 3, pp. 4369–4385, 2020.

[10] W. Chen, M. Hasanipanah, H. N. Rad et al., "A new design of evolutionary hybrid optimization of SVR model in predicting the blast-induced ground vibration," *Engineering with Computers*, vol. 37, no. 9, pp. 1455–1471, 2019.

[11] F. Gong, J. Yan, and X. Li, "A new criterion of rock burst proneness based on the linear energy storage law and the residual elastic energy index," *Chinese Journal of Rock Mechanics and Engineering*, vol. 37, no. 9, pp. 1993–2014, 2018.

[12] M. Hasanipanah, D. J. Armaghani, H. B. Amnieh et al., "Application of PSO to develop a powerful equation for prediction of flyrock due to blasting," *Neural Computing and Applications*, vol. 28, no. Suppl 1, pp. 1–8, 2017.

[13] T. N. Do and T. D. Nguyen, "Prediction of ground surface settlement induced by twin shield tunnellings in urban conditions," *Journal of Mining and Earth Sciences*, vol. 62, no. 2, pp. 47–56, 2021.

[14] H. Xie, J. Zhu, T. Zhou, K. Zhang, and C. Zhou, "Conceptualization and preliminary study of engineering disturbed rock dynamics," *Geomechanics and Geophysics for Geo-Energy and Geo-Resources*, vol. 6, no. 2, pp. 1–14, 2020.

[15] J. Zhao and H. B. Li, "Experimental determination of dynamic tensile properties of granite," *International Journal of Rock Mechanics and Mining SciencesInternational Journal of Rock Mechanics and Mining Sciences*, vol. 37, pp. 861–866, 2000.

[16] F.-Q. Gong and G.-F. Zhao, "Dynamic indirect tensile strength of sandstone under different loading rates," *Rock Mechanics and Rock Engineering*, vol. 47, no. 6, pp. 2271–2278, 2014.

[17] Y. Liu, C. He, S. Wang, Y. Peng, and Y. Lei, "Dynamic splitting tensile properties and failure mechanism of layered slate," *Advances in Civil Engineering*, vol. 2020, Article ID 1073608, 16 pages, 2020.

[18] S. Wang, Y. Liu, K. Du, J. Zhou, and M. Khandelwal, "Waveform features and failure patterns of hollow cylindrical sandstone specimens under repetitive impact and triaxial confinements," *Geomech Geophys Geo-Energy Geo-Resour*, vol. 6, no. 4, p. 57, 2020.

[19] S. Wang, X. Xiong, Y. Liu et al., "Stress–strain relationship of sandstone under confining pressure with repetitive impact," *Geomechanics and Geophysics for Geo-Energy and Geo-Resources*, vol. 7, p. 39, 2021.

[20] Q. H. Wu, X. B. Li, L. Weng, Q. F. Li, Y. J. Zhu, and R. Luo, "Experimental investigation of the dynamic response of prestressed rockbolt by using an SHPB-based rockbolt test system," *Tunnelling and Underground Space Technology*, vol. 93, Article ID 103088, 2019.

[21] X. B. Li, T. S. Lok, J. Zhao, and P. J. Zhao, "Oscillation elimination in the Hopkinson bar apparatus and resultant complete dynamic stress-strain curves for rocks," *International Journal of Rock Mechanics and Mining Sciences*, vol. 37, no. 7, pp. 1055–1060, 2000.

[22] Y. X. Zhou, K. W. Xia, X. B. Li et al., "Suggested methods for determining the dynamic strength parameters and Mode-I fracture toughness of rock materials," *International Journal of Rock Mechanics and Mining Sciences*, vol. 49, no. 1, pp. 105–112, 2011.

[23] Y. H. Huang and S. Q. Yang, "Particle flow simulation of fracture characteristics and crack propagation mechanism of holed-cracked brazilian disc specimen," *Rock and Soil Mechanics*, vol. 35, no. 8, pp. 2269–2277, 2014.

[24] P. H. Bischoff and S. H. Perry, "Compressive behaviour of concrete at high strain rates," *Materials and Structures*, vol. 24, no. 6, pp. 425–450, 1991.

[25] H. M. Dao, A. T. T. Nguyen, T. M. Do, and T. M. Do, "Effect of wetting-drying cycles on surface cracking and swell-shrink behavior of expansive soil modified with ionic soil stabilizer," *Journal of Mining and Earth Sciences*, vol. 61, no. 6, pp. 1–13, 2020.